Article

Controlling Relative Fundamental Crystal Growth Rates in Silicalite: AFM Observation

L. Itzel Meza, Michael W. Anderson, Jonathan R. Agger, Colin S. Cundy, Chin B. Chong, and Richard J. Plaisted

J. Am. Chem. Soc., **2007**, 129 (49), 15192-15201 • DOI: 10.1021/ja0739887

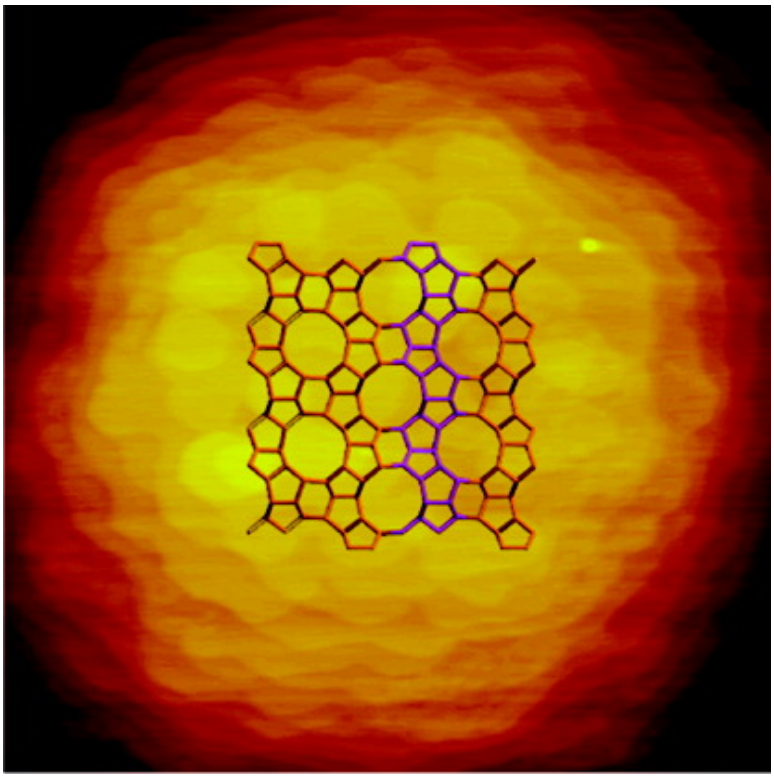

J|A|C|S
ARTICLES
Published on Web 11/14/2007

Controlling Relative Fundamental Crystal Growth Rates in Silicalite: AFM Observation

L. Itzel Meza, Michael W. Anderson,* Jonathan R. Agger, Colin S. Cundy, Chin B. Chong, and Richard J. Plaisted

Contribution from the Centre for Nanoporous Materials, School of Chemistry, The University of Manchester, Oxford Road, Manchester, M13 9PL United Kingdom

Received June 1, 2007; E-mail: M.Anderson@manchester.ac.uk

Abstract: A detailed atomic force microscopy study has been performed on the open-framework, microporous material silicalite. Emphasis has been placed on determining the effect of supersaturation on the crystal growth process. The relative rates of fundamental crystal growth processes can be substantially altered by tuning the supersaturation. In this manner, it is possible to, for instance, switch on and off surface nucleation while retaining terrace spreading. This offers a potential mechanism by which it might be possible to control important crystal aspects such as defect density and intergrowths.

Introduction

Atomic force microscopy (AFM) permits an understanding of crystal growth with a level of detail not possible by other more conventional techniques. AFM has been successfully applied to the study of, for example, proteins, viruses, semiconductors, molecular crystals and open-framework materials. Application to nanoporous open-framework materials is challenging because of a number of aspects. Crystals such as zeolites are generally grown from aqueous media at relatively high temperatures from gel syntheses which are not suitable for *in situ* measurement by atomic force microscopy. Further, crystals formed are often of micron-sized dimension, which makes positioning the AFM tip on a specific crystal facet technically demanding. Consequently, to extract the maximum amount of information about the molecular processes that occur in such systems, it is necessary to adopt a unique experimental strategy. We have consequently designed a set of experiments to achieve our goal for the important open-framework material silicalite. This involves controlling the *ex situ* preparation of the crystals in a specific manner prior to recording the atomic force micrographs. In this work, we have concentrated solely on the effect of supersaturation on the crystal-growth mechanism and associated fundamental growth rates in silicalite. Ultimately, we not only wish to understand the growth mechanism but also to control aspects of the growth so that properties such as, crystal habit, crystal size, defect concentration and template incorporation may be tuned at will. This study yields some important clues as to how supersaturation may be used as a tool to harness such control. This is just a first step but illustrates how, by concentrating on variables one at time, it should be possible to establish the level of understanding required to achieve these goals.

Silicalite is the highly siliceous form of ZSM-5 (structure code MFI), in other words a nanoporous polymorph of silica. Silicalite is a covalently bonded oxide network composed of relatively strong silicon oxygen linkages. These linkages are formed via condensation reactions during crystal growth from an aqueous gel phase. Unlike the dense phase silica polymorph quartz, the structure of silicalite incorporates cages and rings that circumscribe the template molecules (which are in this case tetrapropylammonium cations). Because of the complexity of the silicalite structure in comparison to quartz, the possibility for the incorporation of specific extended defect structures is quite high, as we have reported previously.[1] To minimize the complication from the introduction of such defects, we have chosen a synthetic method that yields single crystals with well-defined crystal habit and low defect concentration. In this manner, it is possible to concentrate on the single variable of supersaturation.

The understanding of crystal growth processes in zeolites has been studied using different microscopy techniques such as AFM, SEM, TEM, and theoretical calculations.[1−16] In general,

(1) Agger, J. R.; Hanif, N.; Cundy, C. S.; Wade, A. P.; Dennison, S.; Rawlinson, P. A.; Anderson, M. W. *J. Am. Chem. Soc.* **2003**, *125* (3), 830−839.
(2) Anderson, M. W.; Agger, J. R.; Thornton, J. T.; Forsyth, N. *Angew. Chem., Int. Ed.* **1996**, *35* (11), 1210−1213.
(3) Sugiyama, S.; Yamamoto, S.; Matsuoka, O.; Honda, T.; Nozoye, H.; Qiu, S.; Yu, J.; Terasaki, O. *Surf. Sci.* **1997**, *377* (1−3), 140−144.
(4) Agger, J. R.; Pervaiz, N.; Cheetham, A. K.; Anderson, M. W. *J. Am. Chem. Soc.* **1998**, *120* (41), 10754−10759.
(5) Anderson, M. W.; Agger, J. R.; Pervaiz, N.; Weigel, S. J.; Cheetham, A. K. Zeolite crystallization and transformation determined by atomic force microscopy. In *Proceedings of the 12th International Zeolite Conference*; Treacy, M. M. J., Marcus, B. K., Bisher, M. E., Higgings, J. B., Eds.; Warrendale: Batimore, MD, 1998; Vol. 3, pp 1487−1494.
(6) Sugiyama, S.; Yamamoto, S.; Matsuoka, O.; Nozoye, H.; Yu, J.; Zhu, G.; Qiu, S.; Terasaki, I., *Microporous Mesoporous Mater.* **1999**, *28* (1), 1−7.
(7) Warzywoda, J.; Valcheva-Traykova, M.; Rossetti, G. A., Jr.; Bac, N.; Joesten, R.; Suib, S. L.; Sacco, A., Jr. *J. Cryst. Growth* **2000**, *220* (1−2), 150−160.
(8) Anderson, M. W.; Hanif, N.; Agger, J. R.; Chen, C.-Y.; Zones, S. I., Atomic force microscopy (AFM) used to relate surface topography to growth mechanisms in SSZ-42. In *Zeolites and mesoporous materials at the dawn of the 21st century*; Galarneau, A., Di Renzo, F., Fajula, F., Vedrine, J., Eds.; Elsevier: Montpellier, France, 2001; Vol. 135, pp 141−148.
(9) Agger, J. R.; Hanif, N.; Anderson, M. W. *Angew. Chem., Int. Ed.* **2001**, *40* (21), 4065−4067.
(10) Sugiyama, S.; Matsuoka, M.; Yamamoto, S. *Microporous Mesoporous Mater.* **2001**, *48*, 103−110.

10.1021/ja0739887 CCC: $37.00

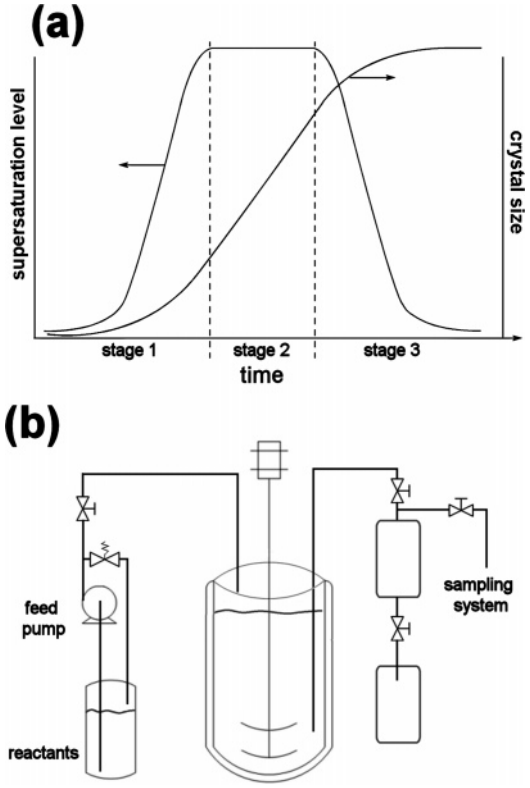

Figure 1. (a) Stages observed during a batch synthesis of a zeolite. (b) Schematic representation of the semicontinuous reactor, not drawn to scale

most of the data obtained from these studies have been acquired from crystals synthesized in batch systems. Such systems can be considered to have three distinctive crystallization stages, as shown in Figure 1a. The first stage comprises the induction period and the initial crystal growth, where the nutrients in the gel become exponentially available. The crystals then follow a linear growth during the second stage, while the supersaturation remains constant at a high level. Finally, the third stage is characterized mainly by the depletion of the nutrients in the gel and a constant crystal size. To date, most of the surface studies conducted on zeolites to understand the crystal growth processes have been carried out by studying crystals that have been recovered from what we have described as the third stage of the synthesis. As a consequence, the surface of the crystals exhibit features related to the last stage of the growth process, where the supersaturation is decreasing rapidly and the crystals size remains approximately constant.

Here we present a study of silicalite crystals obtained from a controlled synthesis characterized by a constant linear crystal growth and high supersaturation level in stage 2 as well as stage 3. The main objective of this work is to provide information from the intermediate stages of zeolite crystal growth and to assess the possibility of influencing crystal growth by means of controlling gel supersaturation during the synthesis.

Experimental Section

Silicalite crystals were obtained from a synthesis carried out in a semicontinuous reactor where experimental parameters were carefully controlled to maintain a constant linear crystal growth. This experiment is part of a study conducted by Cundy et al.[17,18] where the main objective is to control nucleation and crystal growth processes during the synthesis of ZSM-5 and silicalite-1 crystals.

Semicontinuous Flow Reactor. The semicontinuous system, Figure 1b, comprises a polypropylene vessel with working volume of 1 liter. The vessel is fitted with a cap that has inlet and outlet lines for the reagents and the product, respectively. A thermostat bath was used to control the reaction temperature. The mixture in the reactor was stirred at 300 rpm with a stainless steel impeller. A peristaltic pump was used to feed the nutrient into the reactor. Finally, the outlet from the reactor was connected to a sampling system that allows the reactor to keep constant volume and to take homogeneous product slurry that can then be analyzed.

Synthesis of a Series of Silicalite Samples. Five-hundred milliliters of 1.6 μm untwinned seed crystals in their spent mother liquor at a concentration of 9.5 g L^{-1} were placed in the reactor described previously. The temperature was then increased at a constant rate for half an hour to finally reach 130 °C. The reactor was kept at all times under continuous stirring, and then the mixture was allowed to equilibrate for 3 h. After the slurry reached equilibrium, the nutrient feed was switched on.

Seed Crystals. The seed crystals were prepared by following a standard method described by Cundy et al.[19] A gel with a molar composition of 3 Na_2O/60 SiO_2/240 EtOH/6 TPABr/6000 H_2O was used to synthesize lozenge-shaped silicalite-1. NaOH, tetrapropylammonium bromide (TPABr) and tetraethyl orthosilicate (TEOS) were used as the base, template and silica sources, respectively. This mixture was kept at room temperature for approximately 48 h under continuous stirring until a clear solution was obtained. The final gel was then aged for nearly a year. Finally, after raising the base level of the gel from 3 to 8 relative moles of Na_2O, the crystallization was carried out at 130 °C for 48 h. The crystals obtained are about 1.6 μm long in the *z* direction.

Feed Solution. The nutrition feed, with a silicon molarity of 0.48 M and ratios of Si/OH = 8.72 and Si/TPA = 10.0, was pumped continuously into the reactor. The initial feed rate was set to 90 mL h^{-1}, and then it was varied to maintain a constant crystal growth of 0.4 μm h^{-1}.[17] This was achieved by using the following expression: $dx/dt = ku/A$ (a full derivation of the equation is given in Cundy, C. S.; Henty, M. S.; Plaisted, R. J. *Zeolites* **1995**, *15*, 353), where *u* is the mass feed rate, *k* is a constant dependent on crystal geometry and density, *x* is the [001] crystal length and *A* is the total surface area of the crystal population, both at time *t*. Values for *A* were calculated as the reaction progressed by using a computer program that considers known seed crystal size and experimental mass balance. Finally, the feed rates are calculated at different times to maintain the desired crystal growth rate.

Semicontinuous Synthesis. The reaction was continued for a total of 64 h.[17] During this time, samples were taken at specific times to maintain a constant volume inside the reactor. A total of 26 samples were taken from the reaction, and each of them were analyzed to determine the concentration of silica in the gel and in the solution as described briefly later on.[19] During the reaction time, the nutrient feed was stopped for periods of ca. 16 h each at 4.3, 9.6 and 16.4 h. During

(11) Slater, B.; Richard, C.; Catlow, A.; Liu, Z.; Ohsuna, T.; Terasaki, O.; Camblor, M. A. *Angew. Chem., Int. Ed.* **2002**, *41* (7), 1235−1237.
(12) Dumrul, S.; Bazzana, S.; Warzywoda, J.; Biederman, R. R.; Sacco, A., Jr. *Microporous Mesoporous Mater.* **2002**, *54* (1−2), 79−88.
(13) Wakihara, T.; Sugiyama, A.; Okubo, T. *Microporous Mesoporous Mater.* **2004**, *70* (1−3), 7−13.
(14) Warzywoda, J.; Yilmaz, B.; Miraglia, P. Q.; Sacco, A., Jr. *Microporous Mesoporous Mater.* **2004**, *71* (1−3), 177−183.
(15) Meza, L. I.; Anderson, M. W.; Agger, J. R. *Chem. Commun.* **2007**, 2473−2475.
(16) Anderson, W. M.; Agger, J. R.; Meza, L. I.; Chong, C. B.; Cundy, C. S. *Faraday Discuss.* **2007**, *136*, 137−150.
(17) Cundy, C. S.; Henty, M. S.; Plaisted, R. J. *Zeolites* **1995**, *15* (4), 353−372.
(18) Cundy, C. S.; Henty, M. S.; Plaisted, R. J. *Zeolites* **1995**, *15* (5), 400−407.
(19) Cundy, C. S.; Henty, M. S.; Plaisted, R. J. *Zeolites* **1995**, *15* (4), 342−352.

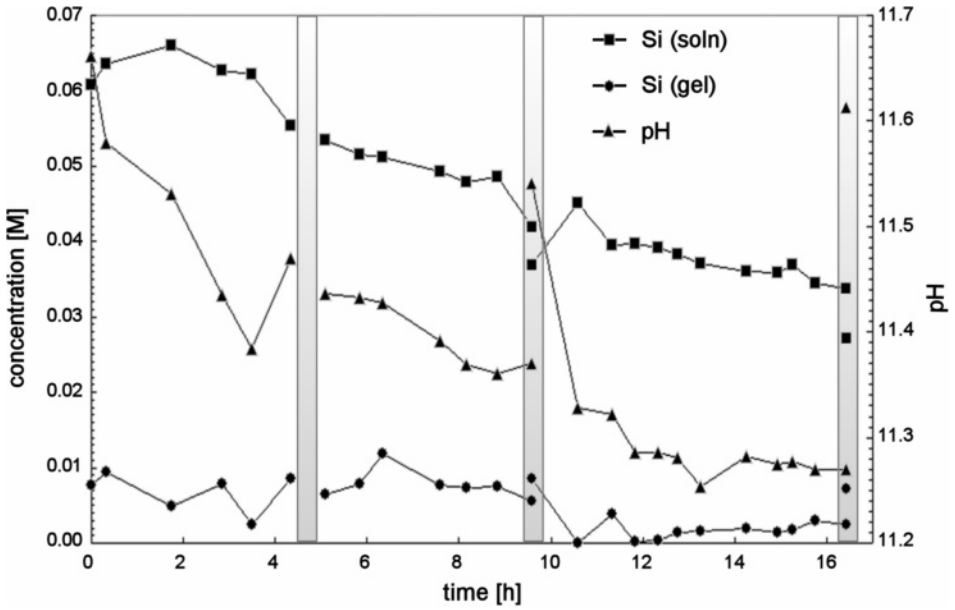

Figure 2. Experimental determination of pH and silica concentration in the gel and solution phases (error on pH readings ±0.02 units, error on concentration ±0.002 M). The gray sections represent periods of 16 h at which the nutrient feed was switched off. The feed was disconnected at 4.3, 9.6 and 16.4 h.[17]

these periods, the reactor was kept at the same reaction temperature (130 °C) and stirring conditions. Samples were taken immediately prior to both switching the feed off and on again the following morning. The reaction times quoted in the present paper refer to the total time in which the feed solution was switched on.

Chemical Determination of Silica. Silica was determined by using molybdic acid reagent, which reacts chemically with monomeric silica. The concentration of silica in gel and in solution was then measured colorimetrically. There exists highly polymeric material for which the rate of depolymerisation to monomeric silica is also determined to complete the analysis. To determine the concentration of silica in solution, a specific volume of the sample is mixed with the molybdate reagent. Then the absorbance is taken after 30 min and the solution silica concentration is obtained. To determine the rate of depolymerisation to monomeric silica, the absorbance is taken periodically during the 30 min following the mixture of the sample and the reagent. In the case of the determination of gel silica, the sample taken is treated with sodium hydroxide at 40 °C while stirring. Then, small volumes of this mixture are taken at different times and added to the molybdate reagent to finally measure the absorbance and determine the concentration of silica. These silica analyses were designed by Cundy et al., and extensive details are described elsewhere.[19]

AFM. Atomic force micrographs were recorded on a Digital Instruments MultiMode with a Nanoscope IIIa controller. Deflection and height images of crystals in air were obtained using AFM contact mode with 0.58 N m^{-1} force constant silicon nitride tips at scan rate of 1 Hz and 512 scans per line.

Modeling. Monte Carlo modeling of crystal growth was performed using a Fortran program written in-house. The program simulates both crystal morphology and surface topography by describing the probability (equivalent to fundamental growth rate) for growth as a function of second-nearest neighbor environment.

Results

Fourteen samples were taken from the semicontinuous reactor and analyzed by means of X-ray diffraction, scanning electron microscopy and atomic force microscopy. The samples were taken at 0, 0.3, 1.7, 2.8, 3.5, 5.0, 7.6, 9.6, 9.6*, 11.8, 13.3 h, 14.9, 16.4 and 16.4* h of reaction after the continuous feed was switched on. Asterisks denote samples removed after periods of 16 h where the nutrient feed was switched off. In other words, the sample 9.6* is equivalent to the sample grown at high supersaturation for 9.6 h followed by a period of 16 h without nutrient feed so that the supersaturation level rapidly dropped as the growing crystals consumed the available silica supply.

Chemical Analysis during Synthesis. Each of the samples taken was analyzed to determine pH, silica concentration in the gel and in the solution. Silicalite crystals were isolated, washed and dried at 105 °C and subsequently characterized. From the chemical analysis carried out to determine silica concentration,[19] the silica in solution comprises mainly monomeric and labile and reactive (i.e., smaller) oligomeric species, whereas the silica found in the gel phase consists of less reactive (i.e., larger) oligomeric and polymeric silicate. The concentration of silica in the gel and in solution and also the pH values observed during the silicalite synthesis are shown in Figure 2. The pH values and solution and gel silica concentrations are observed to gradually decrease as the reaction takes place. After each of the periods where the feed was switched off, the values of the three parameters determined are observed to have higher levels than the ones observed in the samples prior to the switch off of the nutrient feed.

Characterization by XRD and SEM. XRD patterns, shown in the Supporting Information, reveal that all of the samples are highly crystalline. Each of the XRD patterns exhibits all the reflections that correspond to the MFI structure, and there is no indication of any impurities. Scanning electron micrographs reveal that all silicalite crystals exhibit lozenge-shaped morphology, as depicted in Figure 3. All crystals observed also exhibit well-defined {010} and {100} facets. The facets are clearly developed in the seed crystals, and they remain like that throughout the synthesis. The main differences observed during the reaction time are the crystal size and aspect ratio. Some 90° intergrowths were also observed in samples 0.3, 1.7, 9.6* and 16.4.

Crystal Size. The dimensions of the crystals were estimated by measuring the length and width of the {010} and {100} faces. During the time where the nutrient feed was switched on,

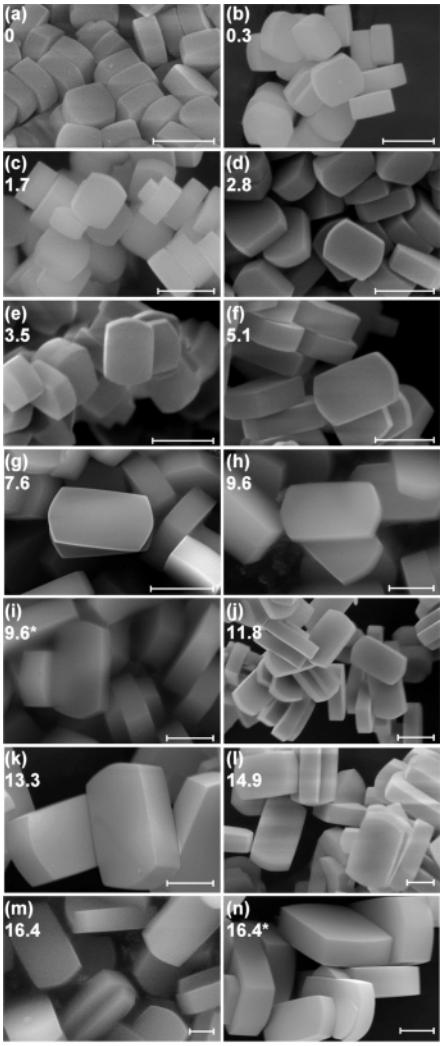

Figure 3. Scanning electron micrographs of the silicalite crystals taken at the different times shown in hours. The scale bar corresponds to 2 mm

silicalite crystals are observed to grow linearly from 3.5 to 16.4 h, as shown in Figure 4a. Prior to this period, there is an apparent stabilization stage between the seed crystals and the nutrient feed. The mean crystal size of the different samples was estimated by considering the length of the crystal along the [001] direction on the {010} faces. Figure 4b shows the mean sizes of each of the silicalite samples. The crystal growth is observed to nearly cease each time the nutrient feed is switched off. Compare crystals taken at 9.6 and 9.6* h and 16.4 and 16.4* h. The growth during this period will be restricted at most to the nutrient remaining in solution when the feed is turned off. The crystals are observed to grow in a fairly constant manner while the nutrient feed is switched on.

Topographic Examination. The silicalite crystals were studied by means of atomic force microscopy to observe differences in surface topography to gain an understanding of the crystal growth process. Here we compare the growth of crystals from two different stages of the crystallization process; first, the intermediate stage where high levels of supersaturation of nutrient are present (defined as high in as much as the crystal exhibits linear growth); second, the final stage in which the gel is depleted as in a normal batch synthesis. These are represented by stage 2 and stage 3, respectively, in Figure 1a.

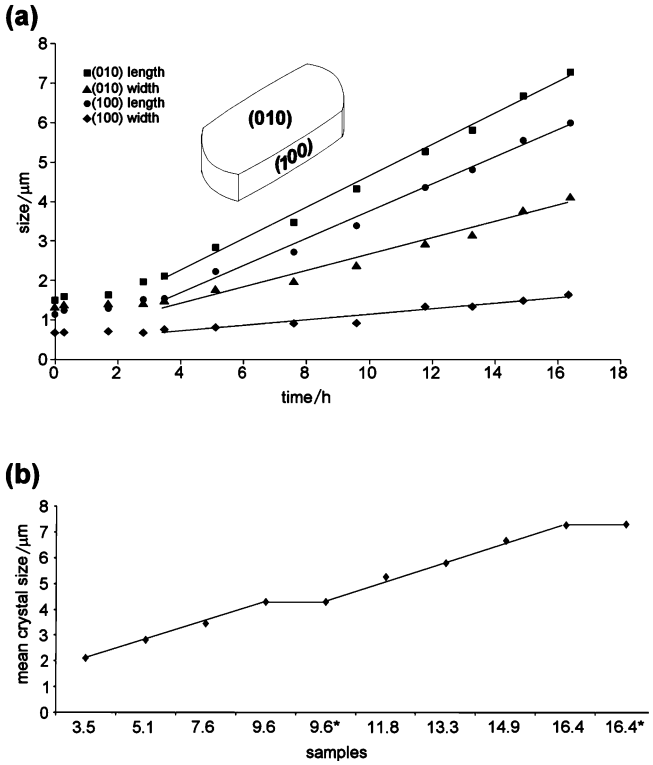

Figure 4. (a) Linear growth observed on the dimensions of the silicalite crystals recovered during period of continuous nutrient feed. (b) Mean crystal size of all the silicalite samples considered for this study (error in crystal size ±0.2 mm).

Figure 5 shows AFM deflection images of the {010} faces of the silicalite crystals. The topography of the seed crystals used for the semicontinuous synthesis is shown in Figure 5a. These crystals exhibit terraces spreading in an isotropic fashion out from the center of the face. The terraces become closer toward the edges of the facet and no significant occurrence of nucleation sites was observed. Figure 5b and c correspond to samples taken after 0.3 and 1.7 h of continuous feed, respectively. The surface features of these crystals remain similar to those of the seed crystal despite the continuous feed being switched on. After 2.8 h, there is a strong effect on the crystal surface topography. Figure 5d shows the surface of a crystal recovered at 2.8 h that is covered with a plethora of small, randomly shaped terraces, which are the result of a high surface nucleation rate. These characteristics persist on the silicalite samples recovered thereafter while the feed was kept switched on, as depicted by crystals taken at 3.5, 5.1, 7.6 and 9.6 h, Figure 5e−h. In all cases, the terrace height is 1.0 ± 0.1 nm.

The nutrient feed was then switched off for a period of 16 h following 9.6 h of reaction. A sample labeled as 9.6* was then taken when the "no feed" period ended. This sample belongs to the final stage of the synthesis where the gel is depleted, stage 3. Figure 5i shows the (010) face corresponding to sample 9.6*. As observed in this image, the surfaces of these crystals exhibit a completely different topography compared to the ones described previously. The surface of the 9.6* crystals shows a low number of nuclei, and the formation and spreading of terraces appears to be the main feature. This formation of pronounced terraces is believed to be the result of multiple nuclei continuing to spread and merging into one another while at the same time new nucleation is suppressed. This is discussed later

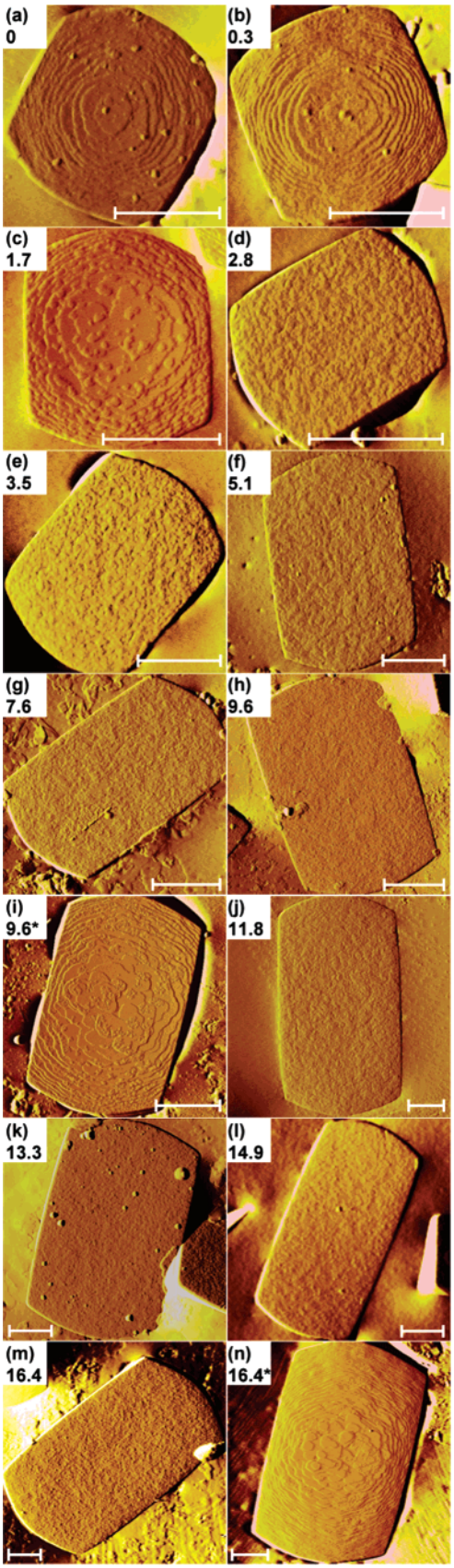

Figure 5. AFM deflection images of {010} faces of the silicalite samples. Crystal shown in (a) corresponds to the seed crystal; (b−h) and (j−m) are crystals that were recovered from the reactor under continuous feed. Crystals shown in (i) and (n) were recovered from the reactor after periods of 16 h where the nutrient feed was switched off and are denoted by 9.6* and 16.4* h. Time expressed in hours. The scale bars represent 1 μm.

in terms of theoretical models of the growth process. The terraces radiate out from the center of the face toward the edges of the facet. As the terraces get closer to the crystal edges, the edges of the terraces align parallel to the edges of the crystal face in the <100> directions, as previously observed for batch synthesized silicalite.[1]

When the feed was switched back on, increasing the level of supersaturation, the topography observed on the crystal faces shows a high nucleation rate as depicted by the AFM images of the crystals recovered at 11.8, 13.3, 14.9 and 16.4 h (Figure 5j−m, respectively). The {010} faces of the crystals in these samples are covered with small randomly shaped terraces, similar in nature to the ones observed previously, each with a height of 1.0 ± 0.1 nm. To finish the reaction, the feed was again discontinued after 16.4 h continuous feed. The last sample was recovered from the reaction after a final period of 16 h with no nutrient feed and the crystals isolated are labeled as sample 16.4*. Figure 5n shows the topography of these final crystals, which is characterized by the spreading of terraces. The surface features observed are similar to the ones described previously for sample 9.6*.

AFM images of the corresponding {100} faces of the different silicalite samples are shown in Figure 6. These images in general mirror the phenomena observed on the (010) faces, except for samples obtained at time 0, 0.3 and 1.7 h. At these short crystallization times, contrary to the clear terraces observed on the counterpart {010} faces, the surface of the {100} facets of these samples exhibits small terraces that have grown from multiple nucleation sites. Although it is still possible to distinguish some terraces edges, the predominant feature is a relatively high level of nucleation.

Summarizing the results described to this point, two types of silicalite crystals were studied: crystals obtained under high supersaturation conditions and crystals recovered from depleted gels. In general, the crystals taken under high supersaturation conditions exhibit a plethora of small terraces covering the {010} and {100} faces of the silicate crystals. On the other hand, the crystals recovered from depleted gels exhibit a significant decrease of the nucleation rate on the crystal faces. This phenomenon is coupled with a terrace spreading process observed on the crystal faces.

To analyze quantitatively the information obtained from the atomic force microscopy, cross sectional analyses were conducted on all the height images obtained from the different silicalite samples. Cross-sectional analysis reveals the height of these terraces to be 1.0 ± 0.1 nm, as can be seen in Figure 7. The small terraces that cover the surface of the crystals recovered under high supersaturation conditions as well as the crystals with clearly developed terraces have the same step heights. In some instances, step heights of ca. 2.0 ± 0.1 nm were observed in the latter crystals. These double-height terraces are a consequence of two terraces with insignificant lateral separation, such as occurs close to the facets edges.

Crystal Surface Analysis. To further understand the crystal growth process of silicalite, sectional analyses were conducted to determine the surface profile on the different facets of the crystals. Additionally, the areas of the {100} and {010} faces were calculated. Regarding the profiles of the faces, those crystals recovered from depleted gels, for instance samples 0, 9.6* and 16.4*, exhibit parabolic profiles. The parabolic nature

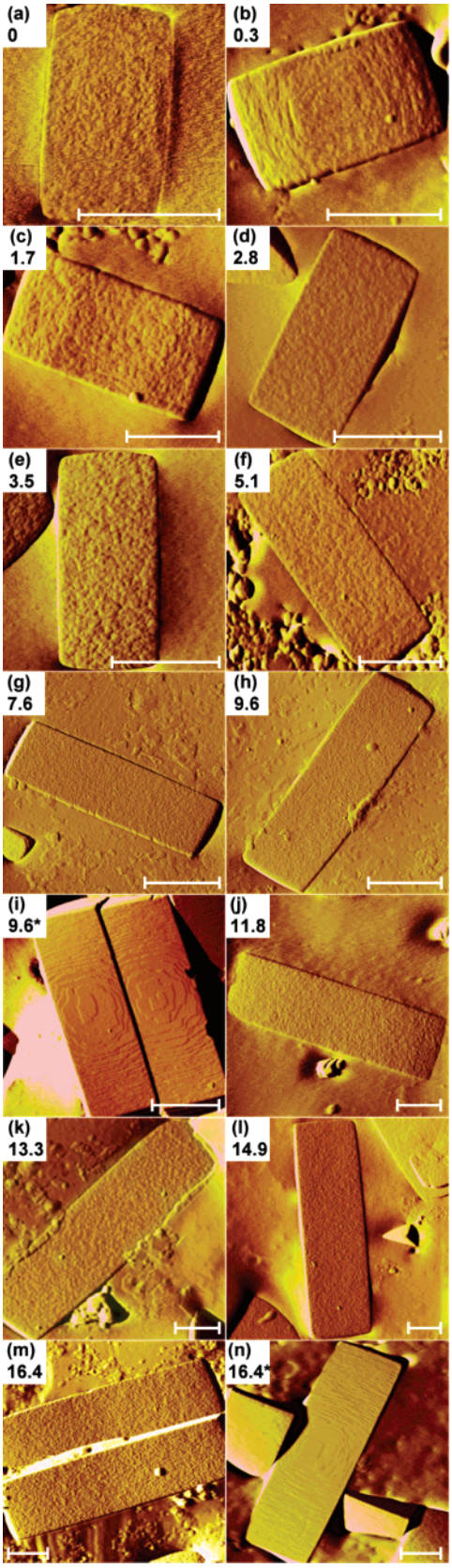

Figure 6. AFM deflection images of {100} faces of the silicalite samples. Letter assignments correspond identically with those of Figure 5. The scale bars represent 1 mm.

is a result of the area of the terraces spreading at a constant rate indicative of a diffusion-limited supply of nutrient to the terrace front. Figure 8 shows cross-sectional analyses taken on

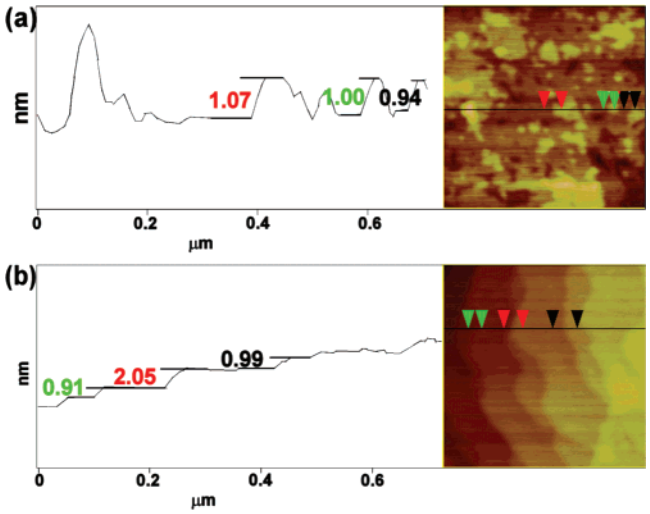

Figure 7. Cross sectional analyses conducted on the surface of the crystals taken (a) under high supersaturation levels and (b) when gel is depleted

the (010) and (100) faces of crystals labeled as 0, 9.6* and 16.4*. Figure 8a and b correspond to the surface profile observed on the seed crystals. The profile observed on the (010) face of these crystals fits perfectly that of a parabola, Figure 8a, whereas the (100) is observed not to have a parabolic profile, Figure 8b. This can be related to the topography information obtained from the deflection AFM images. As shown previously, these seed crystals exhibit terrace spreading on the (010) faces and multiple nucleation on the (100) faces. Crystals taken at 9.6* and 16.4* h show parabolic profiles on both faces, as depicted by Figure 8c−f.

The cross sections match a parabola of the form $y = -ax^2 + b$. The parabolic parameter, a, indicates the degree of bow of the parabola. A series of cross sections were taken from different crystals to calculate an average value of the parabolic parameter for each of the faces from these three samples (0, 9.6* and 16.4*). Table 1 shows the average values of a, which are observed to be very small, and therefore it is not possible to detect any bow on the crystal faces when imaged with a scanning electron microscope. The ratio between the parabolic parameters of the (100) face to the (010) face is ca. 3:1 for crystals 9.6* and 16.4*.

Crystal Area Measurement. The dimensions of the silicalite crystals presented previously in Figure 4a were used to calculate the facet areas. Supplementary Table 2 (which is presented in the Supporting Information) gives the increase in surface areas with time. When the feed is allowed to deplete, the surface area is nearly constant, compare 9.6 with 9.6* and 16.4 with 16.4*. The ratio between the areas obtained from the {010} faces relative to the {100} face was also calculated and presented in Table 2. The ratios calculated for all the samples are observed to increase from ca. 2.4 in the sample labeled as 0 up to a value of 3.4 from sample 16.4*; the relevance of these results is discussed later.

Discussion

The growth process of silicalite crystals has been comprehensively studied by the examination of topographic features on crystals recovered from intermediate and final stages of the synthesis. The silicalite synthesis was closely monitored to keep a linear crystal growth of ca. 0.4 μm h^{-1},[17] as described in the

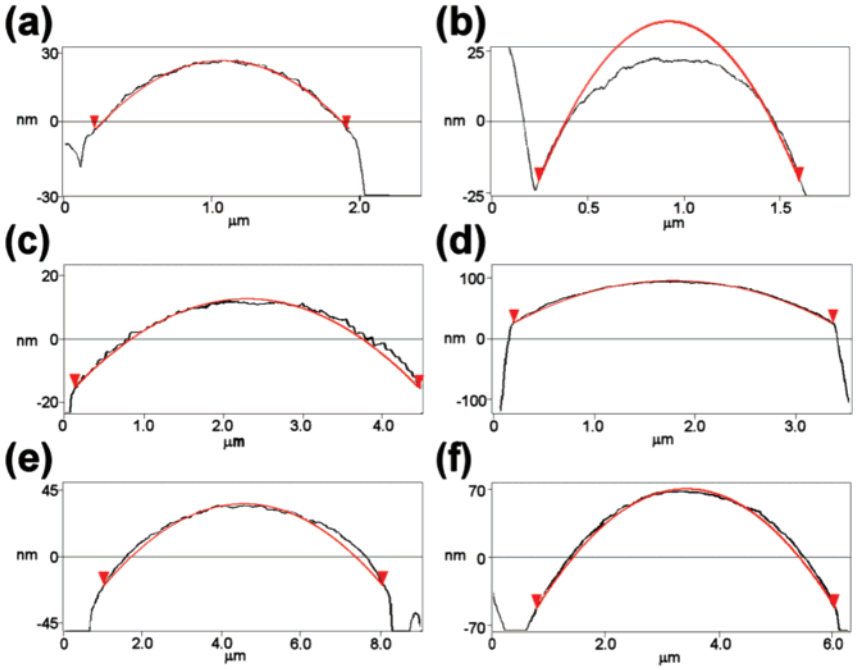

Figure 8. Parabolic profile analysis of the faces of silicalite crystals along the (010) and (100) faces respectively from sample (a−b) 0, (c−d) 9.6* and (e−f) 16.4*. Fitted parabola shown in red.

Table 1. Parabolic Quadratic Parameter "*a*" on the Faces of Silicalite Crystals

	parabolic quadratic parameter $a/\mu m^{-1}$		
silicalite sample	(010)	(100)	ratio of $a_{(100)}/a_{(010)}$
0	0.033 ± 0.001	N/A	N/A
9.6*	0.008 ± 0.001	0.026 ± 0.001	3.26
16.4*	0.005 ± 0.001	0.016 ± 0.002	3.19

experimental procedure. From the parameters monitored during the synthesis, Figure 2, the pH values are observed to decrease throughout the reaction. This could be the result of mineralization of the silica that exceeds the amount of silica attaching to the surface of the silicalite crystals. High pH values are observed after each of the periods where the feed was switched off. This phenomenon can be attributed to the direct effect of the condensation of the silica onto the surface of the crystals and the depletion of the gel. These results appear to be in agreement with the literature,[20,21] where it is observed that high pH values are present when crystalline material is formed. The pH in this system will be the result of the base to silica ratio of the solution which is considered to be in equilibrium with the zeolite crystals.

The dimensions of the crystals were measured to monitor the bulk linear growth rate. The crystals were observed to grow fairly linearly during the crystallization time. This trend was observed to be perturbed each time the nutrient feed was stopped. As previously shown in Figure 4b, there is a halt in crystal growth between crystals taken prior to when the feed was disconnected and the crystals taken after the 16 h of no feed. This can be observed between samples labeled as 9.6 and 9.6*, and samples 16.4 and 16.4*. This phenomenon is a direct consequence of the nutrient feed supply. As long as the feed is switched on, high supersaturation conditions are maintained, and thus, the silicalite crystals grow at a linear rate as expected from the evolution of crystal size and supersaturation presented in Figure 1a. Immediately after the nutrient feed is stopped, the synthesis is observed to behave as the end of a batch synthesis, where the gel supersaturation decreases and the crystals maintain a near-constant size. During this period the nutrients are used by the crystals to develop facets and not for bulk growth. It is possible to repeatedly restart the crystal growth by switching the nutrient feed back on and raising the level of supersaturation.

High surface resolution imaging obtained by atomic force microscopy revealed the surface features of silicalite on the {010} and {100} faces. As shown in Figures 5 and 6, the surface of the crystals taken under high levels of gel supersaturation is covered with multiple terraces as a result of a high nucleation rate. The surface is then observed to drastically change when the nutrient feed is switched off. When the reactor has no continuous feed, the synthesis behaves as the end of a batch system in which the gel depletes. Under these conditions of low supersaturation, surface nucleation has been severely suppressed. It is known from a variety of crystal growth studies that in systems which grow via a layer-by-layer mechanism that the process with the highest activation energy is normally surface nucleation. Terrace spreading phenomena, such as growth at terrace edges, which might be considered as similar to edge or kink sites, will have a substantially lower activation energy. Therefore, these processes will be slowed down at different rates as the supersaturation drops with the nucleation event being the process to be most severely affected. In this case, therefore, the development of substantial terraces after the supersaturation has dropped is a reflection that the terrace spreading processes, although probably slowed, are by no means stopped. Nuclei present on the facets are observed to coalesce into one another and spread.[22] This phenomenon is observed on the AFM images taken from samples labeled as 9.6* and 16.4* shown in images

(20) Casci, J. L.; Lowe, B. M., *Zeolites* **1983**, *3* (3), 186−187.
(21) Lowe, B. M. *Zeolites* **1983**, *3* (4), 300−305.
(22) Burton, W. K.; Cabrera, N.; Frank, F. C., *Philos. Trans. R. Soc. London, Ser. A* **1950**, *A243*, 299−358.

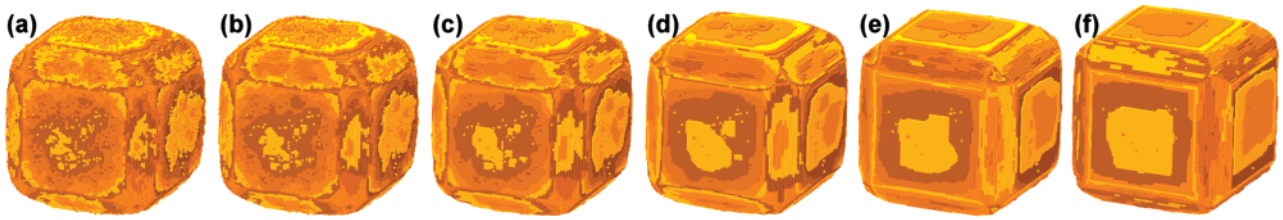

Figure 9. Modeling of the surface topology via a generic Monte Carlo program as a function of relative terrace nucleation and terrace spreading rates. Initial image shows high relative surface nucleation rates equivalent to high supersaturation conditions in Stage 2. The relative rate of terrace nucleation to terrace spreading is then decreased and the simulation continued to mimic the Stage 3 condition of depleting nutrient and falling supersaturation.

(i) and (n), respectively, in Figures 5 and 6. The surface of the {100} and the {010} facets exhibit a low number of nuclei, and terrace spreading appears to be the predominant surface feature. In the case of the seed crystals, time 0 h, and samples taken from the reactor at 0.3 and 1.7 h, the surface features observed seem to be affected by other factors. The seed crystals show terraces spreading on the (010) faces, as expected in a batch synthesis, but the (100) faces are covered by small terraces which have grown from multiple nucleation sites. These features are the result of the (100) facet having a faster growth rate compared to the (010) facet. Regarding samples recovered at 0.3 and 1.7 h, these crystals, despite being obtained from the reactor when the feed was switched on, show terrace spreading on the (010) facets. This is a direct consequence of a period of stabilization between the seed crystals and the new synthesis conditions created by having a continuous flow of nutrient into the reactor.

Zeolite topography and morphology have been studied by means of computational simulations. For instance, Agger et al. have modeled the growth of zeolite A,[9,23] where features such as surface nucleation, terraces spreading, terrace merging and curved terraces were observed. The topography changes observed on zeolite A crystals as a response to supersaturation conditions have recently also been modeled.[24] For instance, at high supersaturation, the facets of zeolite A are observed to be covered with small terraces that are a result of high relative surface nucleation rates. As the supersaturation lowers to an intermediate stage between high and low supersaturation, the formation of surface nuclei decreases in number whereas the terraces already formed on the surfaces are observed to spread and merge into one another. This process requires a slightly higher rate of surface spreading than nucleation and the result is shown in Figure 9.[22] Finally, at low supersaturation, the surface nucleation rate is reduced to almost zero and the terraces are observed to grow out. Such a nonlinear correlation between growing sites and supersaturation is normally dependent on the site type.[25] All previously published AFM images of zeolite crystals exhibit features similar to the ones just described for samples 0, 9.6* and 16.4*.[1−10,12,13,15,16] This is expected since all of those investigations were conducted on crystals that were recovered from the final stage of a batch synthesis.

After the nutrient supply is reconnected, the elevated supersaturation levels cause a resumption of crystal growth and the zeolite surface is once again covered in nuclei. This can be clearly seen by comparing the topographies observed on three consecutive samples, 9.6, 9.6* and 11.8 h as shown in Figure 10. Initially, the crystals taken after 9.6 h of continuous feed have both faces, the {010} and {100}, covered with nuclei, Figure 10a and b. Then, the nutrient supply is stopped for a period of 16 h. During this period the gel supersaturation level decreases and the surface of the crystals 9.6* are observed to develop terrace spreading as depicted by Figure 10c and d. Afterward, the nutrient feed is reconnected and as a consequence, high levels of supersaturation are produced inside the reactor. As a result, high rates of nucleation are registered again and the surface of the crystals is once again covered with nuclei, Figure 10e and f. This process of switching growth on and off

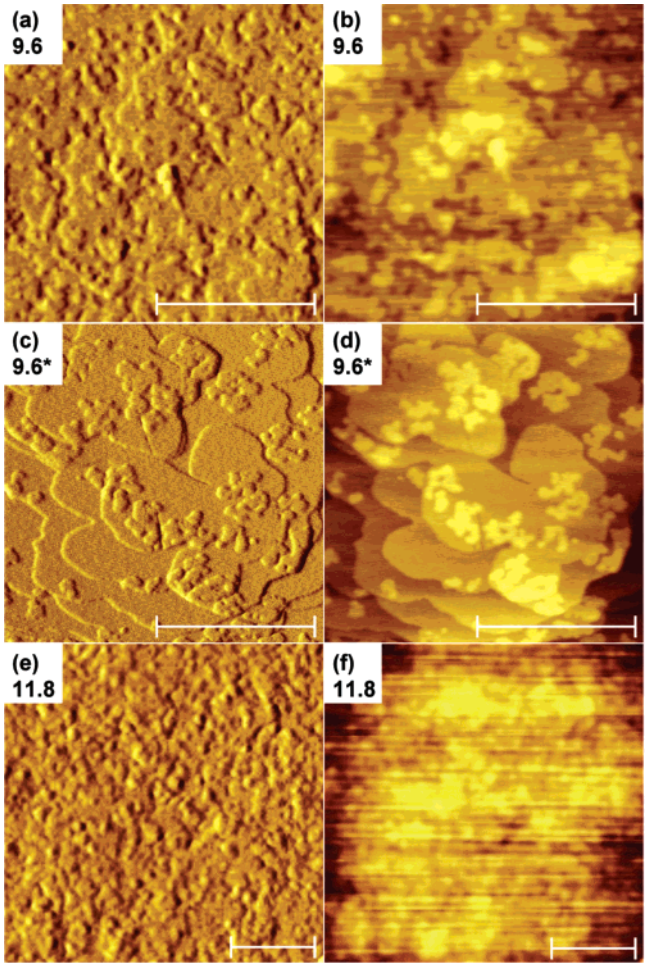

Figure 10. AFM deflection and height images respectively of the (010) face of silicate crystals taken at times shown. Scale bar represents 0.5 mm.

(23) Agger, J. R.; Chong, C. B.; Anderson, M. W. 3D computer simulation of zeolite a crystal growth. In *Recent Advances in the Science and Technology of Zeolites and Related Materials, Pts A−C*; VanSteen, E., Claeys, M., Callanan, L. H., Eds.; Elsevier: New York, 2004; Vol. 154, pp 1282−1288.
(24) Chong, C. B.; Anderson, M. W.; Agger, J. R. Unpublished work, 2007.
(25) Chernov, A. A. *J. Cryst. Growth* **2004**, *264* (4), 499−518.

may be repeated. It is therefore possible to control surface nucleation rates by controlling gel supersaturation levels.

These processes, surface nucleation and terrace spreading, can be correlated to the supersaturation conditions and crystal growth mechanism. Initially, as the supersaturation is increasing, the nucleation process combined with terrace spreading is observed. The surface nucleation rate increases significantly when a high and stable level of supersaturation is reached in the system. At this point, terrace spreading is believed to occur at rates so high they cannot be monitored under the experimental conditions used in this research. Finally, as the supersaturation starts to drop, the surface nucleation process drastically decreases while terrace spreading continues. These processes are a direct result of the relative activation energies, E_a. Surface nucleation is a process that requires higher activation energy than growth associated with terrace spreading. As a consequence, at a high supersaturation, surface nucleation and terrace spreading occur in parallel but at different rates. On the other hand, at low supersaturation, the growth units available in solution do not reach the E_a needed to permit substantial surface nucleation, causing a decrease in the rate of this process. Under these conditions, the surface features observed change as a consequence of the relative increase of growth rate associated with terrace spreading. This also means that the linear dimension of the crystal does not vary significantly during periods of low supersaturation. Similar correlations have been studied on materials such as calcite[26] and adipic acid[27] where AFM has been used to image topography changes at different supersaturation levels.

Detailed examination of the AFM images reveals that the height of the nuclei observed on the surface of the different silicalite samples is ca. 1.0 nm. This height corresponds to the thickness of a pentasil chain, which is in agreement with previous findings (see Figure 11).[1,28,29] The same heights are observed on the crystals which exhibit larger layers as the ones observed on samples 0, 0.3, 1.7, 9.6* and 16.4*.

Finally, to complete the crystal analysis, the surface profile was determined and the areas of the crystals facets were measured. The surfaces of the samples taken when the gel was depleted were found to have a parabolic profile. Such parabolic cross-section implies a constant area deposition, where the overall growth rate of the face will depend principally on the rate of surface nucleation. Parabolic profiles have been seen previously on silicate[1] and zeolite A[4] crystals. Also, Agger et al.[1] found a 4-fold higher rate of nucleation on the (100) face than that on the (010) face of silicate, as given by the parabolic parameters observed on the crystal faces. In the present study, the ratio between the quadratic parameter [a 100 face] to the [a 010 face] is ca. 3:1. This means that the rates of nucleation are higher on the {100} faces than in the {010} for samples 9.6* and 16.4*. The same result is observed in these samples when the areas of the crystals are analyzed. The ratio of areas of the

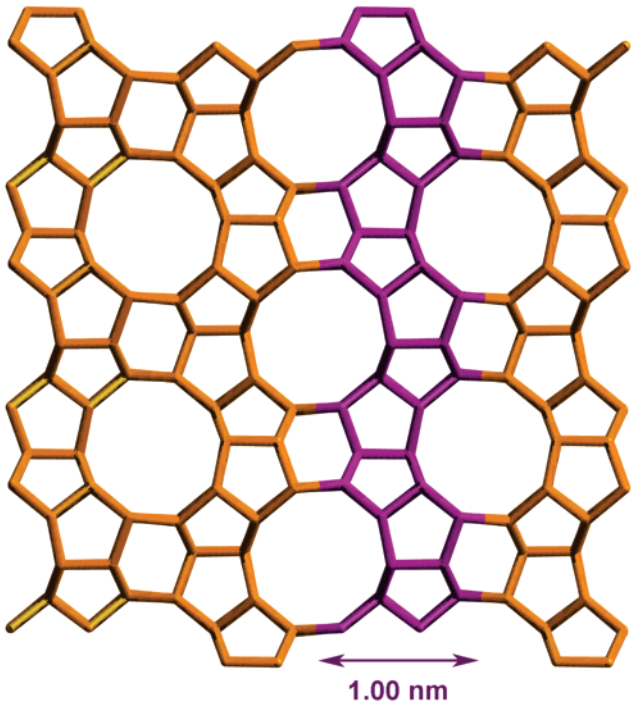

Figure 11. Structure of silicalite viewed along [010] indicating pentasil chain with width 1.0 nm equivalent to all terrace heights observed by AFM.

(010) and (100) facets was found to be ca. 3:1, as shown previously in Table 2, implying a 3-fold ratio in their growth rates, with the (010) being the slower growing face. In other words, the growth rate on the (100) face is faster than on the (010) face, and therefore, the (010) face is larger than the (100).

The ramifications of the ability to control the relative rates of surface nucleation versus terrace spreading are that it may be possible to control both defects and intergrowths in open-framework materials via this approach. For crystals that grow by a layer upon layer mechanism, there is often a choice for the orientation of a nucleating layer. If there is a high nucleation density caused by a high surface nucleation rate relative to the terrace spreading rate then there will be high probability that different nucleation sites create terraces with different orientation. When these terraces spread and merge, a defect will be created at the junction. To reduce the density of such defects it will be necessary to increase the rate of terrace spreading relative to surface nucleation. In this manner, a low density of surface nuclei will be formed that will spread across the entire crystal surface and not encounter another terrace. Conversely, by increasing the relative rate of surface nucleation with respect to terrace spreading the defect density could be maximized, if such property were desired. Such situation exists in materials such as silicalite, faujasite and the microporous titanosilicate ETS-10.

Conclusions

This work demonstrates that it is possible to control the relative rates for fundamental growth processes in the open framework material silicalite by careful control of the supersaturation. Surface nucleation can be switched on and off repeatedly in response to changes in supersaturation. Atomic force microscopy has revealed that the activation energies

(26) Teng, H. H.; Dove, P. M.; De Yoreo, J. J. *Geochim. Cosmochim. Ac.* **2000**, *64* (13), 2255−2266.
(27) Keel, T. R.; Thompson, C.; Davies, M. C.; Tendler, U. B.; Roberts, C. J. *Int. J. Pharm.* **2004**, *280* (1−2), 185−198.
(28) Diaz, I.; Bonilla, G.; Lai, Z.; Terasaki, O.; Vlachos, D. G.; Tsapatsis, M. Silicalite-1 crystals with modified morphology: HRTEM imaging and synthesis of B-oriented films. In *Recent Advances in the Science and Technology of Zeolites and Related Materials, Pts A−C*; Elsevier: New York, 2004; pp 1160−1167.
(29) Diaz, I.; Kokkoli, E.; Terasaki, O.; Tsapatsis, M. *Chem. Mater.* **2004**, *16* (25), 5226−5232.

associated with surface nucleation and terrace spreading are such that one process can be switched off in preference to the other. This is important because defects are often incorporated into open framework materials as a result of insufficient terrace spreading rates relative to surface nucleation rates. This work, therefore, opens up the possibility to control defect concentrations through subtle control of the synthetic conditions.

Acknowledgment. Thanks to Ayako Umemura for assistance in rendering the theoretical simulations.

Supporting Information Available: Structural information of silicalite, Powder XRD characterization patterns and areas of the silicalite samples measured from SEM images. This material is available free of charge via the Internet at http://pubs.acs.org.

JA0739887